

## STABILITY OF UV ILLUMINATED DYE SENSITIZED SOLAR CELLS (DSC) STUDIED BY PHOTOINDUCED ABSORPTION IN THE SECOND RANGE

Katrine Flarup Jensen<sup>1,2</sup>, Henning Brandt<sup>1</sup>, Chan Im<sup>2</sup>, Jürgen Wilde<sup>3</sup>, Andreas Hinsch<sup>1,\*</sup>

<sup>1</sup> Fraunhofer Institute for Solar Energy Systems (ISE), Heidenhofstrasse 2, 79110 Freiburg, Germany

<sup>2</sup> Konkuk University- Fraunhofer Next Generation Solar Cell Research Center (KFnSC), 120 Neungdong-ro, Gwangjin-gu, Seoul 143-701, Korea

<sup>3</sup> Department of Microsystems Engineering – IMTEK, University of Freiburg, Georges-Köhler-Allee 103, 79110 Freiburg, Germany

### Corresponding author

\*) *Andreas Hinsch, Tel: +49-76-14588-5417, Fax: +49-761-4588-9000, Email: andreas.hinsch@ise.fraunhofer.de*

**ABSTRACT:** In this work we present a method to test the stability of dye-sensitized solar cells (DSC) exposed to UV. Photoinduced Absorption (PIA) in the second range was applied to dyed- and undyed cells with a 405 nm probe laser. The pump source was a UV diode with an intensity of approximately 100 x the suns UV content. PIA was used to determine the influence of UV on the DSC cell for dyed and undyed cells. With this highly sensitive setup, we have shown the influence of H<sub>2</sub>O in the electrolyte, which causes faster triiodide depletion. We found that this method is very suitable to test the purity of electrolyte and, more generally, the DSC tolerance towards UV illumination. The method can be applied to optimize the device life time. A comparison to cells which have been aged in a UV chamber was made, where faster degradation of DSC cells with H<sub>2</sub>O in electrolyte was also observed.

**Keywords:** Dye-Sensitized, Degradation, Spectroscopy, Stability, TiO<sub>2</sub>

## 1 INTRODUCTION

The dye-sensitized solar cell (DSC) imitates nature's photosynthesis by the principle of a light-absorbing dye chemically adsorbed on mesoscopic TiO<sub>2</sub> [1, 2]. The charge separation of the photoexcited electron occurs at the interface between the dye and the mesoporous semiconducting TiO<sub>2</sub>, and charge is transported in the TiO<sub>2</sub> by diffusion. A redox couple iodide/triiodide (I<sup>-</sup>/I<sub>3</sub><sup>-</sup>) electrolyte reduces the oxidized dye molecule and is reduced back at the catalytic platinumized counter electrode, see figure 1.

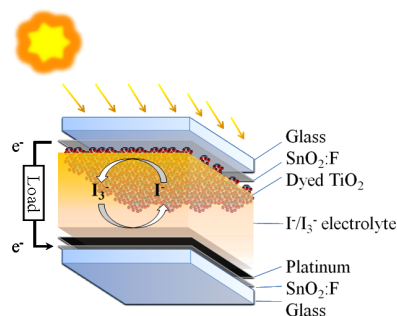


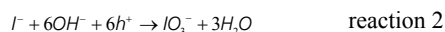
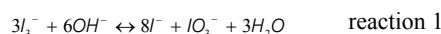
**Figure 1:** Working principle of the dye-sensitized solar cell (DSC)

The long-term stability of the DSC is influenced by the intrinsic and the mechanical stability as well as the operation conditions. Depletion of I<sub>3</sub><sup>-</sup>, also known as electrolyte bleaching, can affect the electrical performance of the DSC if the cell becomes I<sub>3</sub><sup>-</sup> diffusion limited [3].

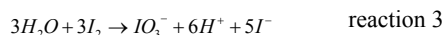
An undesired degradation mechanism occurs due to UV illumination, which is caused by electrolyte bleaching. It is well known that TiO<sub>2</sub> in the anatase form becomes photocatalytic for wavelengths below 390 nm. The absorption of UV light generates electron-hole pairs in the TiO<sub>2</sub>. In the complete DSC, the TiO<sub>2</sub> is covered by a monolayer of dye molecules which should prevent the TiO<sub>2</sub> photocatalysis. But in reality UV illumination has been

observed to cause degradation by slow photocatalysis in the DSC caused by a reaction between triiodide and oxidized impurities by e.g. formation of iodate IO<sub>3</sub><sup>-</sup> [4-7]. The photooxidized impurities represent an unwanted side reaction with the redox pair of the electrolyte as the released electron will deplete the triiodide concentration by reduction to iodide.

If the electrolyte contains H<sub>2</sub>O and has a pH between 5 and 9, triiodide and iodate can co-exist (reaction 1), but if the pH is above 9, iodate is more likely to form than triiodide (reaction 2) [8].



If H<sub>2</sub>O is present in the cell, protons (H<sup>+</sup>) will be released during UV illumination along with IO<sub>3</sub><sup>-</sup> production [9] due to reaction 3.



Reaction 3 has also been proposed as a thermally activated process, which can occur under thermal ageing in the dark at elevated temperatures [10]. So triiodide depletion in not stabilized DSC cells does not only occur due to UV illumination. Therefore it is likely that precautions like cell protection with a UV foil, cannot prevent the electrolyte bleaching in DSCs containing some impurities. In the following UV illumination is used to accelerate the reactions causing electrolyte bleaching.

At reverse bias, the platinumized counter electrode works as a cathode and the voltage drop at the pt/electrolyte interface can be high enough to reduce H<sup>+</sup> and produce H<sub>2</sub> causing bubble formation and large vapor pressure in the cell [9, 11]. This high voltage drop at the pt/electrolyte interface particularly occurs when the cell is I<sub>3</sub><sup>-</sup> diffusion limited.

The scope of our work was to create a setup for fast detection of the electrolyte response to UV illumination. This method is suited for understanding the causes of the electrolyte bleaching and, specifically to test the purity of the electrolyte.

## 2 EXPERIMENTAL

### 2.1 Cell preparation

The cells were fabricated on so called master plates [3], with 5 individual cells (active area of 5 cm x 0.5 cm) on a soda lime glass with a transparent conductive oxide TCO ( $\text{SnO}_2\text{:F}$ ,  $8\Omega/\square$ , Pilkington).

The substrates were laser scribed for electrical isolation of the individual cells and filling holes in the counter electrode glass were drilled. The substrate was subsequently cleaned by mechanical cleaning with detergent, ultrasonification for 15 min at 70 °C, rinsing in DI water followed by 2 min ultrasonification and cleaning with acetone, ethanol and dried with  $\text{N}_2$ . The cells were fabricated by screen printing of the active layers. Ag paste (Ferro) as current collector,  $\text{TiO}_2$  paste (Dyesol DSL 18 NR-T) on the photoelectrode, nano-platinum paste (3D-Nano) on the counter electrode and glass frit as sealant material (based on a  $\text{ZnO-SiO}_2\text{-Al}_2\text{O}_3$  composition) were printed on the electrodes with intermediate drying at 150 °C in a conveyor belt oven between every printing step. The plates were sintered at a maximum temperature of 565 °C which resulted in a  $\text{TiO}_2$  layer thickness of 12  $\mu\text{m}$ . Afterwards the electrodes were positioned and fused for hermetic sealing in a fusing oven resulting in a plate distance of 20  $\mu\text{m}$ .

For the investigation, DSC cells with and without adsorbed N719 dye were fabricated. The cells were dyed with 0.27 mM N719 (Dyesol) in absolute ethanol by purging the dye solution through the cell for 24 hours. The cells were rinsed with acetonitrile and dried with nitrogen.

The redox electrolyte contained 0.1 M iodine (Sigma-Aldrich), 0.1 M guanidine thiocyanate (Sigma-Aldrich), and 0.50 M n-butyl-1H benzimidazole (NBB) (Merck) dissolved in 1-methyl-3-propylimidazolium iodide (PMIM-I) (Merck, Germany) with 11 wt % acetonitrile (Sigma-Aldrich). This electrolyte will be referred to as PMII-electrolyte in the following. Demineralized water was used to create redox electrolyte with 5 wt %  $\text{H}_2\text{O}$ . The dilution resulted in an iodine concentration of 0.093 M.

The PMII electrolyte with no added water was filled in the cells in the glovebox, while the water-containing electrolyte was filled in ambient atmosphere. The filling holes were sealed with Surlyn 1702 (DuPont) and a thin slide glass.

### 2.2 Photoinduced absorption spectroscopy setup

The setup, figure 2, consists of a probe laser at 405 nm. A Si photodetector is used to detect the transmitted light. In order to make the setup sensitive, a light-absorbing tube was placed at the inlet of the photodetector, to ensure that no scattered light was detected. The pump beam is a UV diode, with an intensity of approximately 100 x the UV part of the solar spectrum 1 sun, AM 1.5.

The pump beam was applied for 40 seconds, starting at 10 s. During the experiment, the voltage from the photodetector was measured which corresponds to the transmittance of the cell at 405 nm. The cell was kept at open circuit during the measurement and the photovoltage of the cell was also measured.

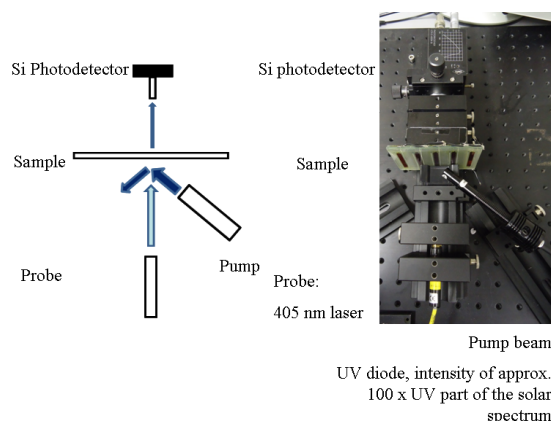


**Figure 2:** Setup for photoinduced absorption (PIA) spectroscopy of the DSC.

### 2.4 UV vis spectrophotometry

The absorbance of respectively a TCO glass ( $\text{SnO}_2\text{:F}$ ), a dyed cell with PMII electrolyte and an undyed cell with PMII electrolyte were measured with the UV-vis-NIR Varian Cary 500 Spectrophotometer. The baseline was ambient air.

### 2.5 UV Chamber

Dyed cells were aged in a UV chamber (Dr. Gröbel, Germany) with homogeneous distribution of UVA (300-400 nm), with an intensity of approximately 2 x the UV part of the solar spectrum 1 sun, AM 1.5.

### 2.6 Electrical characterization

The cells were electrically characterized by cyclic voltammetry (CV) with the electrochemical workstation IM6 (Zahner Electric). CV was conducted under illumination of a sulfur lamp setup of approx. 0.8 Sun [3], scan rate 40 mV/s in the range [0.75V;-0.1V]. The cell temperature was 45 °C.

Electrical Impedance Spectroscopy (EIS) was measured under illumination and at  $V_{OC}$  with 10 mV amplitude in the frequency range of 100 kHz to 100 mHz. The one-diode model was used for fitting the EIS results [12].

## 3 RESULTS

### 3.1 From transmittance to absorbance

The photodetector signal [V] was correlated to transmittance, T, by using a filter glass with known transmittance at 405 nm. A photodetector signal of 1 V was determined to correspond to a T of 0.5086% for the measurements.

The Beer-Lambert Law gives the relation between absorbance, A, and transmittance, T [13], eq. 1:

$$A = -\log_{10}[T] \quad \text{eq. 1}$$

Absorbance is linearly proportional to the concentration of absorbing species c, eq. 2:

$$A = \epsilon \cdot l \cdot c \quad \text{eq. 2}$$

$\epsilon$  is the molar extinction coefficient [L/(mol cm)],  $l$  is the diffusion length and  $c$  is the concentration of absorbing species.

The Beer-Lambert Law was used to calculate absorbance from the measured photodetector signal, and the ratio in absorbance change  $\Delta A$  at time  $t$  is given by:

$$\Delta A = A_t : A_{t=0} \quad \text{eq. 3}$$

The absorbance spectrum of a TCO substrate with  $\text{TiO}_2$ , a dyed cell with PMII electrolyte and an undyed cell with PMII electrolyte is shown in figure 3. It is seen that at 405 nm, both the dye and electrolyte are absorbing, and the  $\text{TiO}_2$  also shows absorbance. The photos below in figure 3 display the samples which were measured with the PIA setup.

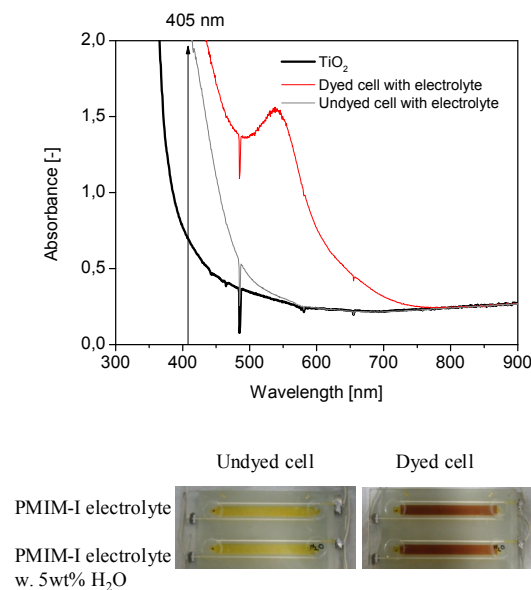


**Figure 3:** Absorbance spectrum of TCO glass and  $\text{TiO}_2$  (-), dyed cell with electrolyte (-), undyed cell with electrolyte (-)  
Master plate cells: Undyed and dyed cell with respective PMII-electrolyte and PMII-electrolyte with 5 wt %  $\text{H}_2\text{O}$  measured with the PIA setup.

### 3.2 Photoinduced absorption spectroscopy

The influence of the probe beam was determined by carrying out the measurements with and without the 405 nm laser. From figure 4a) it is seen, that the 405 nm laser generates an open-circuit voltage of 0.18V in the undyed cell (-). So electron-hole pairs are generated in the  $\text{TiO}_2$  when the cell is illuminated by the probe laser. The cell voltage is zero when the probe laser is turned off (-◇-).

The UV diode generates a photovoltage of 0.6 V, independently of whether the probe laser is turned on (-) or not (-◇-), so significantly more electron-hole pairs are generated due to the strong UV diode.

The photodetector signal (-) increases from 1.7 V to 2.7 V after the UV diode is turned on, corresponding to an increased transmittance at 405 nm. When the UV diode is turned off, the photodetector signal decreases slowly accompanied with an increase in photovoltage induced by the probe laser.

The measurement without the probe laser shows, that the cell voltage decreases to zero after the UV diode is turned off (-◇-).

The influence of the dye is shown in figure 4b), where a similar measurement is carried out. The probe beam generates a photovoltage of 0.4V (-) because the dye absorbs at this wavelength. When the UV diode is on, the cell reaches a voltage of 0.55V. After the diode is turned off, the voltage elapses back to the initial cell voltage induced by the probe laser. In the experiment where the probe laser is turned off, the cell voltage (-◇-) follows same behaviour as described for figure 4a).

The photodetector signal for the dyed cell (-), figure 4b) is lower than seen for the undyed cell, as the dye absorbs the 405 nm probe light. A decrease in photodetector signal is seen for the time (0-10 s) which indicates that the dye excitation at 405 nm generates triiodide. When the UV is turned on, the photodetector signal increases from 0.02 V to 0.033 V, indicating bleaching of the electrolyte. When the UV diode is turned off, the photodetector signal decreases rapidly compared to the figure 4a) of the undyed cell to below the initial voltage of the photodetector.

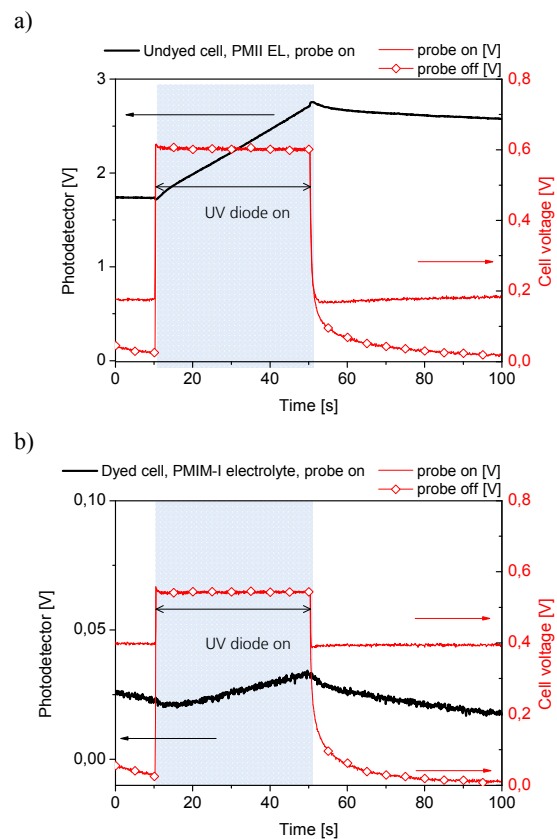


**Figure 4:** (-) Photodetector signal [V] related to transmittance, (-) cell voltage when 405 nm laser is on during the measurement, (-◇-) cell voltage when 405 nm laser is turned off during measurement.  
a) PIA measurement of undyed  $\text{TiO}_2$  cell with PMII electrolyte.  
b) PIA measurement of dyed cell with PMII electrolyte (-)

Cells with electrolyte containing 5 wt %  $\text{H}_2\text{O}$  were further measured. In figure 5a) it is seen that the 405 nm laser generates a voltage in the undyed cell (-) similar to the same cell with no added  $\text{H}_2\text{O}$ , figure 4a). The UV

diode now causes the cell voltage to reach 0.65V ((-) and (-◊-)). The photodetector signal (-) increases after the UV diode is turned on from 5.2 V to 10.4 V, which is significantly higher than seen in figure 4a). This is attributed to the lower concentration of triiodide caused by the addition of H<sub>2</sub>O, hence a lower electrolyte light absorption. The increase in photodetector signal corresponds to an increased transmittance at 405 nm caused by the UV exposure.

The influence of the dye is shown in figure 5b) for the H<sub>2</sub>O-containing dyed cell. The probe beam generates a voltage of 0.48V (-), and when the UV diode is on, the cell reaches a voltage of 0.65V ((-) and (-◊-)). The voltage in the water-containing dyed cell are higher than as seen in figure 4b), which is discussed in section 3.3. The UV diode causes the photodetector signal to increase from 0.05 V to 0.16 V. As seen in figure 4b), the photodetector signal decreases again after the UV diode is turned off, due to the regenerative production of triiodide caused by the dye excitation at 405 nm.

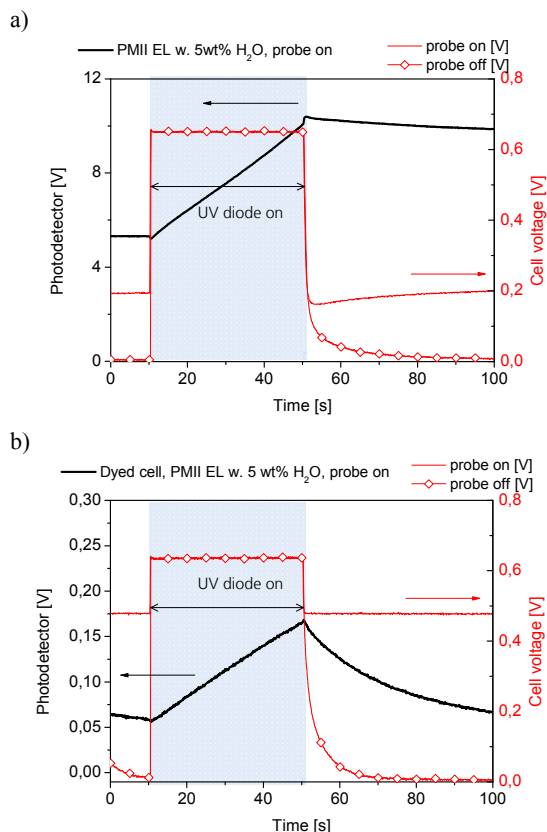


**Figure 5:** (-) Photodetector signal [V] related to transmittance, (-) cell voltage when 405 nm laser is on during the measurement, (-◊-) cell voltage when 405 nm laser is turned off during measurement.  
**a)** PIA measurement of undyed cell with PMII electrolyte with 5 wt%.  
**b)** PIA measurement of dyed cell with PMII electrolyte with 5 wt% H<sub>2</sub>O.

The ratio in absorbance change,  $\Delta A$  eq. 3, of the undyed cells is shown in figure 6a). It is seen that  $\Delta A$  becomes negative when the UV diode is turned on, showing that the UV exposure causes a decrease in triiodide concentration.  $\Delta A$  stays relatively stable after the UV diode is turned off. The largest change in A is seen for the H<sub>2</sub>O-containing cell reaching 0.91, compared to 0.95 for the cell with no added

H<sub>2</sub>O.

$\Delta A$  of the dyed cells is shown in figure 6b). As  $\Delta A$  already shows a slope in the time 0-10s where only the probe beam is on, triiodide is generated. It is seen that  $\Delta A$  becomes negative when the UV diode is turned on, so the UV exposure causes a decrease in triiodide concentration. The regeneration of triiodide after the UV laser is turned off can partially be explained by the disturbing photovoltaic effect caused by the probe laser.

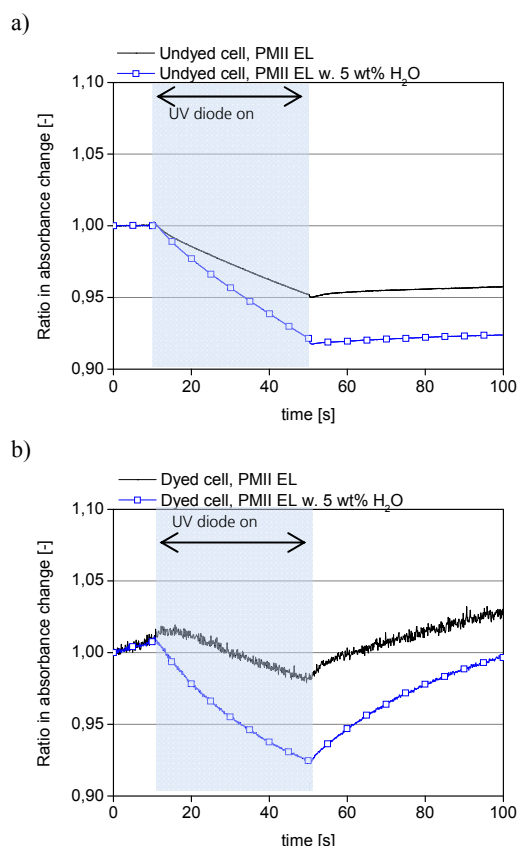


**Figure 6:** **a)** Ratio of absorbance change  $A_t:A_{t=0}$  of the undyed cell with PMII electrolyte(-), and the cell with 5 wt% H<sub>2</sub>O in electrolyte (-) **b)** Ratio of absorbance change  $A_t:A_{t=0}$  of the dyed cell with PMII electrolyte (-), and the cell with 5 wt % H<sub>2</sub>O in electrolyte (-).

It is clear, that the largest UV-induced change in absorbance occurs for cells containing electrolyte with addition of 5 wt% of H<sub>2</sub>O. Since the cells with ‘non-aqueous’-electrolyte also show a response to the UV illumination, it is possible that the electrolyte was not impurity-free. Even though the electrolyte was prepared in the glovebox, it seems that the residual water content was sufficient to induce UV-related electrolyte bleaching in the cells.

### 3.3 Cells aged in UV chamber

Dyed cells were placed in a UVA chamber (approx. 2x the UV part of the solar spectrum) [10], with a cell temperature of approximately 40°C.

Figure 7a) shows the photocurrent density-voltage ( $j_{sc}$ , V) characteristics for the cell with no added water in PMII the electrolyte. It is noticeable that the initial fill factor is bad. This is correlated to the Nyquist plot, figure 7b) where the high-frequency semicircle corresponding to the charge-transfer resistance at the pt electrode ( $R_{ct}$ )



overlaps with the semicircle representing the recombination resistance at the  $\text{TiO}_2$ -dye-electrolyte interface [2, 11, 12]. For extended time of UV ageing, the  $j_{sc}$  decrease which is connected to the decrease in triiodide concentration and thus an increase in  $R_{ct}$  and electrolyte diffusion resistance,  $R_d$ . After 241 h's of UV ageing, the cell is almost completely electrically passivated, all triiodide is lost and the  $R_{ct}$  is greatly increased.

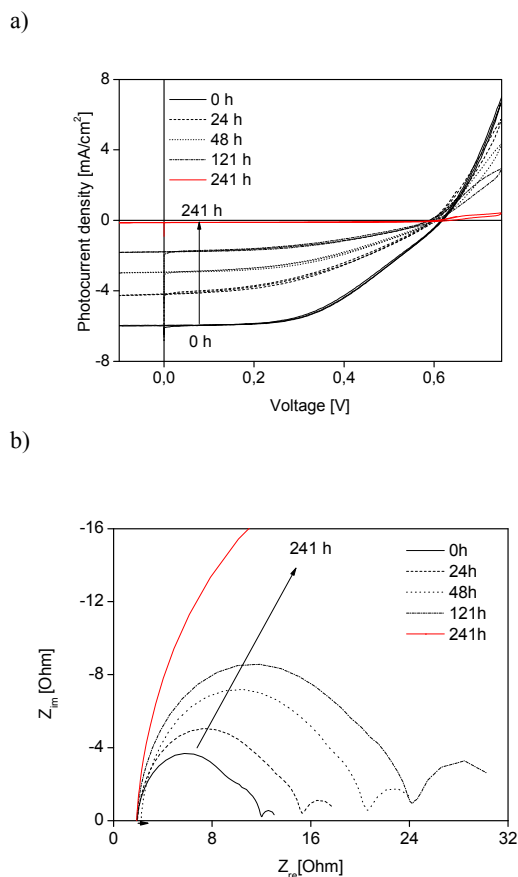


**Figure 7:** Dyed DSC cell aged in UV chamber. Electrolyte with no added  $\text{H}_2\text{O}$ . **a)** CV. Scan rate: 40mV/s, **b)** EIS.

In figure 8, the results of the UV aged cell with 5 wt %  $\text{H}_2\text{O}$  in electrolyte are shown. The addition of  $\text{H}_2\text{O}$  improves the fill factor and also increases the  $V_{OC}$ , figure 8a). As seen from figure 8b) the  $R_{ct}$  is significantly lower than as seen in figure 7b) which could indicate that the  $\text{H}_2\text{O}$  has a cleaning effect of the platinum electrode, which could have been contaminated during the dye purging. The UV ageing initially causes the  $j_{sc}$  to increase and the  $V_{OC}$  to decrease, but between 48 h and 121 h's of UV exposure, the cell becomes completely passivated due to triiodide depletion which is complimented by a huge increase in  $R_{ct}$ .

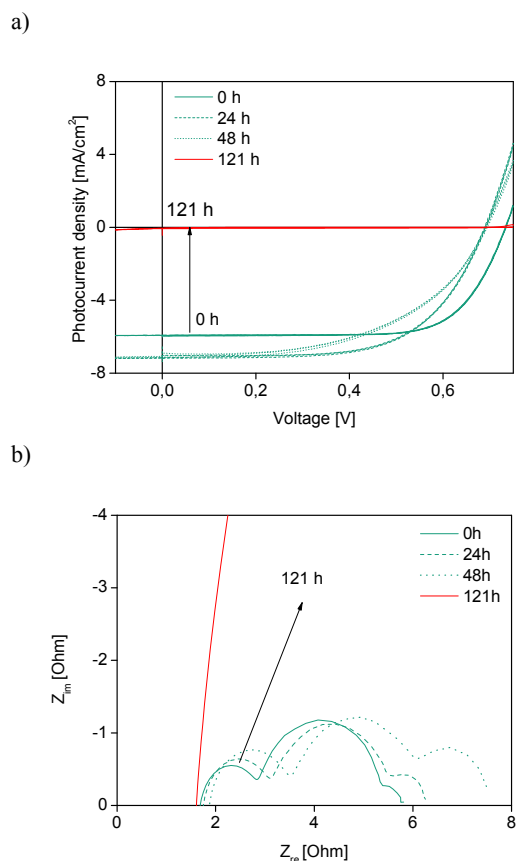


**Figure 8:** Dyed DSC cell aged in UV chamber. Electrolyte with addition of 5 wt%  $\text{H}_2\text{O}$ . **a)** CV. Scan rate: 40mV/s, **b)** EIS.

The cell with added water in the electrolyte became electrically passivated significantly faster than the cell with no addition of  $\text{H}_2\text{O}$ . The triiodide depletion was hypothesized by reaction 2 and 3 where triiodide reacts into iodate under UV and in presence of  $\text{H}_2\text{O}$  in the electrolyte.

The results show that  $\text{H}_2\text{O}$  content has detrimental influence on the DSC stability during UV illumination. Even the cells with no added water degraded under UV so it is doubtful if the electrolyte was completely water-free or contained other impurities.

## 4 DISCUSSION

### 4.1 Comparison between PIA measurements and ageing in UV chamber

The results obtained with the PIA setup showed a greater change in UV-photoinduced for the cell with a significant amount of  $\text{H}_2\text{O}$ . This result points towards a reduced lifetime of the cell under UV illumination. A faster UV-degradation of cells with  $\text{H}_2\text{O}$ -containing electrolyte was shown by monitoring the electrical performance of cells aged by UV in a UV chamber. The cell with 5 wt %  $\text{H}_2\text{O}$  in electrolyte failed in less than half the time as the cell with 'non-aqueous' electrolyte.

### 4.2 Pre-treatment of electrolyte

The results clearly show that water should be avoided in the electrolyte. Therefore a method to pre-treat the electrolyte for driving out  $\text{H}_2\text{O}$  should be found. We are

currently investigating thermal and electrochemical methods to pre-treat the electrolyte for removal of H<sub>2</sub>O before introducing it into the cell.

13. J. D. J. Ingle and S. R. Crouch, *Spectrochemical Analysis*, Prentice Hall, New Jersey, NJ, USA, 1988.

## 5 CONCLUSION

We have developed a setup based on photoinduced absorption, to study the UV stability of the DSC under strong exposure of UV from a spot diode. Photoinduced absorption in the second range with a probe laser at 405 nm was used to determine the influence of UV on the DSC cell for dyed and undyed cells. This approach can be used to test the purity and UV stability of various electrolytes.

By comparing the PIA results with electrical characterization of dyed cells aged in a UV chamber, it is clear that H<sub>2</sub>O content in the electrolyte has detrimental influence on the DSC stability during UV illumination and should be prevented.

## 6 ACKNOWLEDGEMENTS

This work is supported by Seoul Metropolitan Government in the Joint Project KU/Fraunhofer-ISE Next Generation Solar Cell Research Center (KFnSC) between Konkuk University, Republic of Korea, and Fraunhofer ISE, Germany (Seoul R&BD Program no. WR090671).

The authors would like to thank Dr. Simone Mastroianni and Welmoed Veurman from Fraunhofer ISE for helpful discussions.

## 7 REFERENCES

1. B. O'Regan, M. Grätzel, *Nature* **335**, 737-740 (1991).
2. A. Hinsch, W. Veurman, H. Brandt, R. A. Loayza; K. Bialecka, K. F. Jensen, *Prog Photovolt Res Appl* **20**, 6, 698-710 (2012).
3. A. Hauch, A. Georg, *Electrochim. Acta* **46**, 3457-3466 (2001).
4. A. Hinsch, J. M. Kroon, R. Kern, I. Uhlendorf, J. Holzbock, A. Meyer and J. Ferber. *Prog Photovolt Res Appl* **9**, 425-438 (2001).
5. H. G. Agrell, J. Lindgren, A. Hagfeldt, *Solar Energy* **75**, 169-180 (2003).
6. M. Carnie, D. Bryant, T. Watson, and D. Worsley, *Int J Photoenergy*, Article ID 524590, doi:10.1155/2012/524590 (2012).
7. B. Macht, M. Turrion, A. Barkschat, P. Salvador, K. Ellmer, H. Tributsch, *Sol. Energ. Mat. Sol. Cells* **73**, 163-173 (2002).
8. R. Abe. *Bull. Chem. Soc. Jpn.*, **84**, 1000-1030 (2011).
9. S. Mastroianni, A. Lanuti, S. Penna, A. Reale, T.M. Brown A. Di Carlo, and F. Decker, *ChemPhysChem* **13** 2925-2936 (2012).
10. R. Sastrawan, "Photovoltaic modules of dye solar cells," Dissertation, University Freiburg Freiburg, Germany, 2006 <http://www.freidok.uni-freiburg.de/volltexte/2623/pdf/Sastrawan>
11. Photovoltaic modules of dye solar cells Dissertation.pdf. K. Flarup Jensen, W. Veurman, H. Brandt, C. Im, J. Wilde, A. Hinsch. *MRS Online Proceedings Library*, 1537, mrss13-1537-b11-14 doi:10.1557/opl.2013.790.
12. L. Han, N. Koide, Y. Chiba, A. Islam, T. Mitate. *Comptes Rendus Chimie* **9**, 645-651 (2006).